TECHNO-ECONOMIC ANALYSIS AND OPTIMIZATION OF A HYDROGEN REFUELING STATION INTEGRATED IN A RENEWABLE-BASED MICROGRID

Roberta Tatti[1]*, Mario Petrollese[1], Giorgio Cau[1]

[1]University of Cagliari, Department of Mechanical, Chemical and Material Engineering, Cagliari, Italy

*Corresponding Author: roberta.tatti@unica.it

ABSTRACT

The transportation sector is one of the most responsible of CO_2 emissions globally. To mitigate greenhouse gas emissions in this sector, vehicles powered by alternative energy sources with almost zero climate impact during their use, such as green electricity or hydrogen, are spreading more and more rapidly.
In this context, this paper investigates the feasibility of integrating a hydrogen refueling station within a microgrid that includes a dedicated photovoltaic plant coupled with a battery bank and by the presence of a hydrogen production and storage system. The purpose of the study is finding the optimal design of the microgrid in order to produce and supply high pressure hydrogen to satisfy the daily demand of a fleet of hydrogen buses, which would substitute diesel buses in the local public network.
Specifically, an optimization problem has been implemented in Matlab and solved using a genetic algorithm for two different microgrid configurations; Green Hydrogen Production and Mixed Hydrogen Production. The optimization sought to determine the optimal sizes for the microgrid components, i.e. the photovoltaic system, the batteries, the hydrogen generator and the low and high pressure storage tanks. The optimization was studied according to two objective functions: the maximization of self-sufficiency of the microgrid and the minimization of hydrogen production costs.
The results showed that designing a microgrid able to guarantee a complete self-sufficiency results in a significant rise in the hydrogen production costs (a LCOH equal to 25 €/kg was found for the case of Green Hydrogen Production and 29 €/kg for the case of the Mixed Hydrogen Production). Otherwise, considering the values obtained in both cases with the same LCOH and total SSR, it was found that starting from an LCOH of 22.12 €/kg the best EMS is the Green-EMS, which guarantees a renewable SSR of 99.25% against 93.21% of the Mixed-EMS. The values found are higher than the LCOH achieved by powering the hydrogen generator only with the grid (equal to about 13 €/kg). This result highlights the additional costs deriving from the requirement of storage systems, in order to guarantee the actual production and use of green hydrogen. However, this is also the case characterized by greater CO_2 emissions (532 t CO_2/year vs 52 t CO_2/year for the Mixed-EMS and no GHG emissions for the Green-EMS).

1 INTRODUCTION

The transport sector is one of the most polluting globally, accounting for 20% of global CO_2 emissions in 2020. Of these emissions, 77% are due to road transport and in particular to passenger cars, responsible of 51% of emissions (Bahou, 2023). Similar percentages characterize Europe, were total CO_2 emissions related to the transport sector have contributed for 28.6% in 2020 (Pang *et al*., 2022). From a mobility point of view, future energy sources for vehicles should predominantly be electricity or hydrogen (Logan et al., 2020).
The diffusion of Battery Electric Vehicle (BEV) has increased significantly in recent years, together with the development of proper charging stations. However, looking at hydrogen vehicles, the still few available hydrogen refueling infrastructures, contextually to high hydrogen prices, are nowadays the barriers to the diffusion of Fuel Cell Electric Vehicles (FCEVs) (Maestre *et al*., 2023). In this regard, by 2030, EU member States objective is to install a charging station for BEVs every 60 km

https://doi.org/10.52202/077185-0008

and a Hydrogen Refueling Station (HRS) for FCEVs every 100 km along the trans-European transportation network (Cardona *et al*., 2023).
As electric vehicles, BEVs and FCEVs have different features. In both cases, propulsion is ensured by an electric motor: in BEVs using the electricity stored in the on-board battery, typically a lithium-ion battery (Lawrence *et al*., 2023), while in FCEVs using electricity generated onboard by a fuel cell powered by compressed hydrogen and using oxygen from the atmosphere (Förster *et al*., 2023). However, BEVs have several disadvantages, such as the shortage of certain raw materials and critical minerals for the manufacture of batteries, like lithium, nickel or cobalt, or the incompatibility of using batteries for heavy duty, maritime or air freight applications, as long routes might impact the operations of BEVs with limited battery capacity (Coppola *et al*., 2023). As BEVs, FCEVs have not pollutant emissions during their use, and only generate steam (Micena *et al*., 2020). However, if the electricity used directly in BEVs and that used to produce hydrogen for FCEVs is generated from fossil fuels, the environmental benefits become negligible. An actual mitigation of GHG emissions can be therefore achieved only if electric vehicles are fueled from renewable energy vectors. Focusing on HRSs, these are complex systems with several variable designs. Hydrogen can be produced on site near the station or off site in a centralized hydrogen plant and transported using pipelines, ships, trucks, etc. The on-site HRS can be further categorized into off-grid and on-grid according to the connection or not to the grid of the hydrogen production system. Regarding the production costs of green hydrogen these are between 2.5-5.5 €/kg (Kakoulaki *et al.*, 2021), a value similar to that indicated by Mallapragada *et al.* (2020). Slightly higher costs ranging between 2.6-12.3 $/kg were found by Guerra *et al.* (2019), as well as by Schnuelle *et al.* (2020) (4.33-12.38 $/kg).
Several studies have been carried out about the integration of HRSs in different microgrid systems, characterized by Photovoltaic (PV), Wind Turbines (WT) and/or Battery Storages (BS). Cardona *et al.* (2023) focused their study on a HRS powered by solar PV, with the aim of producing hydrogen at 350 bar and 700 bar. Bahou (2023) studied an on-site HRS powered by PV and electric grid, with the aim of study the replacement of local taxi fleets with hydrogen vehicles. Gökçek and Kale (2018) studied two different microgrid systems (WT+PV+BS and WT+BS), optimizing all the components to obtain the lowest Levelized Cost of Hydrogen (LCOH). A similar optimization was carried out by Förster *et al*. (2023), which studied a microgrid integrated with a HRS and an electric vehicle charging station, and by Pang *et al*. (2022), which focused on an off-grid HRS aimed to satisfy the electrical, heating and cooling demand. Finally, a multi-objective study was proposed by Lawrence *et al*. (2023), where an on-site HRS powered by a PV-WT system was optimized in order to minimize the LCOH and maximize the system's reliability. Different studies have also been conducted on bus fleet replacement: Coppola *et al*. (2023) focused on a life cycle assessment of a local bus fleet replacement in Italy, while Maestre *et al*. (2023) studied a similar case in Spain, considering all type of vehicles to be replaced with only hydrogen ones.
In this context, this study focuses on the modeling and optimization of a renewable-based microgrid integrated with an on-site HRS to allow the replacement of some diesel buses of a local bus line with hydrogen ones. The main objectives of the study concern:

- the development of a mathematical model in MATLAB to study the performance of the renewable based microgrid for different Energy Management Strategies (EMSs), characterized by an increasing share of green hydrogen production;
- the optimization of the system design according to two different objective functions: the maximization of the Self-Sufficiency Ratio (SSR) of the renewable-based microgrid and the minimization of the LCOH, in order to find the best size for the microgrid components;
- the determination of the additional costs deriving from the requirement of storage systems to guarantee the actual production and use of green hydrogen compared to the hydrogen production costs obtainable by powering the hydrogen generator only with the public grid and the calculation of CO_2 emissions for each EMS.

2 SYSTEM CONFIGURATION

The renewable-based microgrid considered in this study is characterized by a PV system coupled with a BS and a hydrogen production and storage system, composed of a Hydrogen Generator (HG), a Low

https://doi.org/10.52202/077185-0008

Pressure Hydrogen Tank (LP-HT), a Hydrogen Compressor (HC) and a High Pressure Hydrogen Tank (HP-HT) for the storage of gaseous hydrogen at 450 bar. As shown in Figure 1, the considered microgrid is also connected to the Public Grid (PG), in order to study two different EMSs, characterized by an increasing share of renewable energy used for green hydrogen production, compared finally to the hydrogen production costs obtainable by powering the HG only with the public grid. The purpose of the microgrid concerns the supply of high-pressure hydrogen (350 bar) to a given number of heavy duty vehicles, in this specific case hydrogen buses.

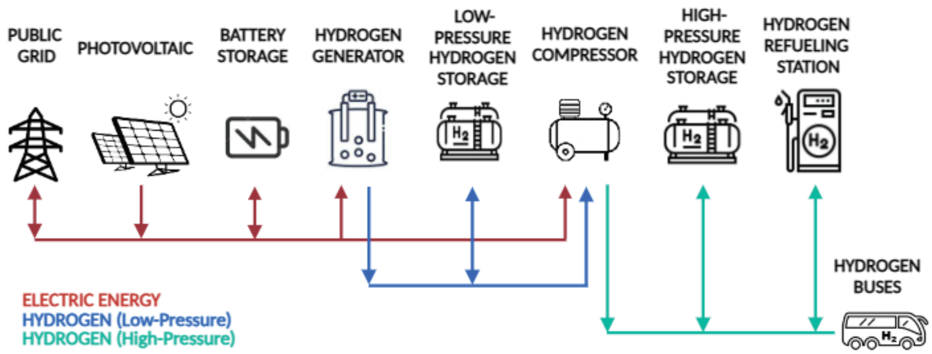

Figure 1: Schematic system of the renewable-based microgrid proposed

The substitution of six diesel buses with FCEVs in a given line of the local public network of the city of Cagliari (Italy) is considered as case study. The characteristics of the bus integration are reported in Table 1. It is assumed that the buses will be refueled every day at two different times throughout the day: considering that the refueling time for one bus is around 10 minutes, the first three buses will be refueled at 6 am, while the others at 1 pm, in order to make them available on the road at 7 am and 2 pm respectively. The hydrogen demand for each refueling is therefore 36.45 kg (1 435.6 kWh, referring to the Higher Heating Value). As regards the CO_2 emissions of the local bus company, these amount to 1.072 kg CO_2/km: consequently, considering the same number of roundtrips, the emissions avoided by replacing the 6 diesel buses with hydrogen vehicles correspond to 284.46 t CO_2/year.

Table 1: Characteristic of hydrogen bus fleet (Fragiacomo *et al*., 2022)

Parameter	Value	Parameter	Value
Bus autonomy	350 km	Line roundtrip length	24.3 km
Bus hydrogen tank capacity	35 kg	Commercial velocity	13.3 km/h
Bus hydrogen tank pressure	350 bar	Total line distance for 1 bus per day	121.5 km
No. of buses	6	H_2 for all buses per day (ref. HHV)	72.9 kg
Total No. of full per day (year)	6 (2 184)	H_2 for all buses per year (ref. HHV)	26 535.6 kg

3 MATHEMATICAL MODELS

The microgrid performance in a typical year were evaluated through a mathematical model developed in MATLAB. The user need was modeled using a daily hydrogen load, according to the data reported in Table 1. In the following, the mathematical models implemented for evaluating the expected performance of each component of the considered system will be described.

3.1 PV system

The PV generation profile was simulated starting from a typical meteorological year dataset of the location considered obtained by Meteonorm Software (Meteonorm, 2022) The PV system is composed of modules characterized by a peak power of 355 Wp (SUNPOWER, 2024), while the overall size is considered a design parameter to be optimized. Regarding the PV plant orientation, an

https://doi.org/10.52202/077185-0008

azimuth angle of -30° and a tilt angle equal to 30° were considered. The output power P_{PV} of the PV subarray was calculated by Equation (1):

$$P_{PV}(t) = P_{PV,nom} \frac{GI(t)}{GI_{NOCT}} \left[1 + \gamma \left(T_C(t) - T_{C,STC}\right)\right] \eta_{INV}\, f_{PV} \quad (1)$$

where the incident radiation (GI_{NOCT}) was assumed equal to 800 W/m^2, the Cell Temperature under Standard Test Conditions ($T_{C,STC}$) is set equal to 25°C, the PV temperature coefficient (γ) is -0.0027 1/°C, the inverter efficiency (η_{INV}), is given by the manufacturer as a function of the PV power output. Other secondary losses, like wiring losses, shading, soiling of the modules and aging are accounted in a derating factor f_{PV} equal to 0.9. The Global Irradiance (GI) and the operating Cell Temperature (T_C) were calculated using the method proposed by Duffie & Beckman, 2013.

3.2 Battery storage

The energy stored in the BS was evaluated by determining its state-of-charge (SOC_{BS} in Equation (2)), which indicates the ratio between the amount of stored energy and the nominal storage capacity:

$$SOC_{BS}(t) = SOC_{BS}(t-1) + \frac{\left[P_{BC}(t)\eta_{BC} - \frac{P_{BD}(t)}{\eta_{BD}}\right] \Delta t}{E_{BS}} \quad (2)$$

where P_{BC} is the power input during charging phase and P_{BD} is the power output during discharging phase. The batteries efficiency during charging and discharging phases (η_{BC} and η_{BD}) were set equal to 98% and 97% respectively, since the batteries are lithium type, while the applied time step (Δt) and the battery depth-of-discharge were assumed equal to 1 h and 80% respectively. The battery capacity (E_B), as for the PV system, is a design parameter to be optimized.

3.3 Hydrogen section

The hydrogen section includes a HG, a LP-HT, in which hydrogen is stored up to the HG delivery pressure (while the minimum pressure is set equal to 4 bar, equal to the minimum working pressure of the HC), a HC and a HP-HT (characterized by nominal pressure of 450 bar to guarantee the refueling of the buses at 350 bar). The size of the HG and the capacity of both HTs were considered design parameters to be optimized during the performance analysis.
Concerning the HG, a commercial electrolyzer based on the Proton Exchange Membrane (PEM) technology, with a hydrogen production of 1 Nm^3/h at 35 barg, was considered. According to the manufacturer specification (Serra *et al.*, 2020), it was assumed that the HG can operate in a range between 20% and 100% of its rated power. The HG often operates in off-design mode with variable efficiency, as the PV power supplying the hydrogen section and the user needs are time dependent. Therefore, the hydrogen mass flow rate $\dot{m}_{HG}$ produced by a given HG power supply P_{HG} depends on the electrolyzer efficiency η_{HG} (Serra *et al.*, 2020), given by Equation (3):

$$\eta_{HG}(t) = \frac{\dot{m}_{HG}(t)\, HHV_{H_2}}{P_{HG}(t)} \quad (3)$$

where HHV_{H_2} is the Higher Heating Value of the hydrogen. The HC is a three-stage volumetric compressor with intercooling to avoid high temperatures in case of immediate sending of hydrogen to the HRS. The hydrogen flow rate to be compressed resulted from the energy balance of each management strategy, while the power was calculated with Equation (4), where i indicates the compressor stage, with the volumetric and isentropic efficiencies ($\eta_{v,i}$ and $\eta_{is,i}$) calculated with the equations proposed by P.C. Hanlon (2001), as a function of the pressure ratio.

$$P_{HC_i}(t) = \frac{\dot{m}_{HC}(t) \cdot \left[h_{out,i}(t) - h_{in,i}(t)\right]}{\eta_{v,i}(t) \cdot \eta_{is,i}(t)} \quad (4)$$

https://doi.org/10.52202/077185-0008

Finally, the energy stored inside the LP-HT and HP-HT at a given time was evaluated based on the relative state-of-charge, (SOC_{LP-HT} and SOC_{HP-HT}) determined by Equation (5) and Equation (6) respectively:

$$SOC_{LP-HT}(t) = SOC_{LP-HT}(t-1) + \frac{[\dot{m}_{HG}(t) - \dot{m}_{HC}(t)]\, HHV_{H_2}\, \Delta t}{E_{LP-HT}} \quad (5)$$

$$SOC_{HP-HT}(t) = SOC_{HP-HT}(t-1) + \frac{[\dot{m}_{HC}(t) - \dot{m}_{HRS}(t)]\, HHV_{H_2}\, \Delta t}{E_{HP-HT}} \quad (6)$$

where $\dot{m}_{HG}$, $\dot{m}_{HC}$ and $\dot{m}_{HRS}$ are the hydrogen mass flow rate produced by the HG, compressed by the HC and used by the HRS respectively, while E_{LP-HT} and E_{HP-HT} are the hydrogen storage capacities expressed in energy terms of the LP-HT and HP-HT, respectively. Equations (5) and (6) allows to evaluate the energy converted by the hydrogen generator and stored in the LP-HT and that stored in the HP-HT after hydrogen compression.

3.4 Energy management strategy

A detailed Energy Management Strategy (EMS) for the analyzed microgrid was implemented in MATLAB, with the aim to study the system performance and to optimize the sizing of the microgrid components. Specifically, two different EMSs were investigated: a Mixed Hydrogen Production EMS, in which the hydrogen generator can be fed by the PV+BS system but, if necessary, also by the electricity purchased from the grid, and a Green Hydrogen Production EMS, in which the hydrogen generator is powered only by the PV and by the energy stored in the BS, with energy purchased from the grid exclusively in case of need for the HC. Looking at the mixed case, as shown in Figure 2, the EMS is divided in four different parts.

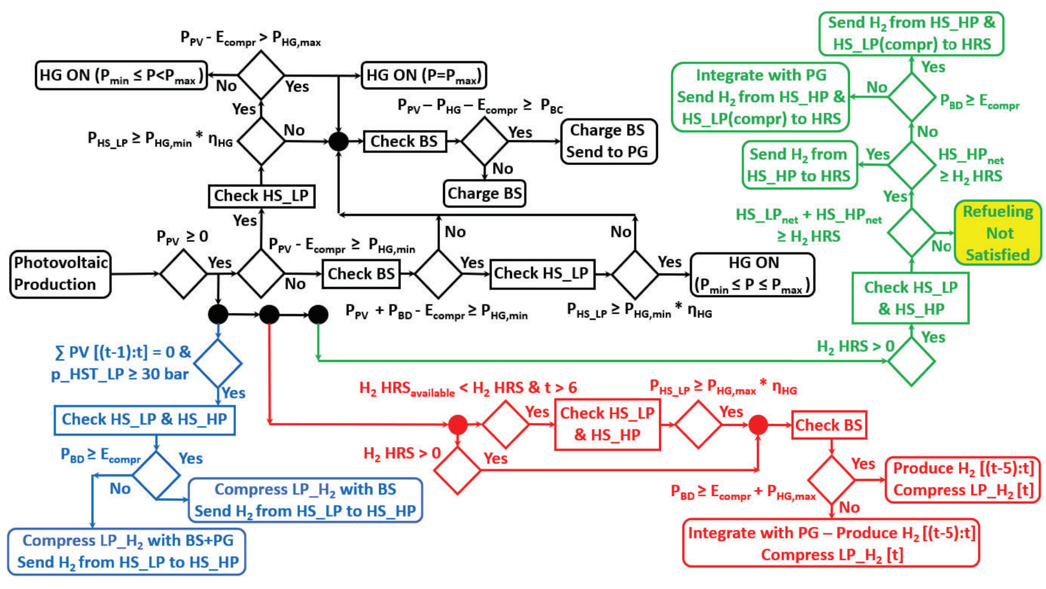

Figure 2: Energy management strategy scheme of the mixed hydrogen production case

The black part shows the logic activated for the production of green hydrogen, so using energy only from PV, from PV+BS or only from BS. The green part represents the calculation of the hydrogen stored in both HTs. Particularly, the HRS request is satisfied with the hydrogen stored in the HP-HT, which can be partially or fully supported by the hydrogen stored in the LP-HT after compression. The compression is also carried out when the PV system is not producing energy and the LP-HT is almost

https://doi.org/10.52202/077185-0008

fully charged (over 30 bar on 35 bar), as indicated in the blue part, with energy from BS or from the grid. Finally, the red part concerns the hydrogen production with energy from the grid, planned in case there is a deficit compared to the HRS's request. In particular, a check is carried out on both HTs five hours before the scheduled refueling time (6am and 1pm). If the quantity of hydrogen available, including that expected to be produced in the following five hours by energy from PV, is less than that requested by the HRS, the hydrogen deficit will be covered by energy from the grid.
In the case of green hydrogen production, EMS is similar to the previous one. In particular, the black part (hydrogen production from PV and/or BS) and the green part (calculation of the hydrogen available for the HRS) are equal, while in this case hydrogen production with energy from the grid is not allowed (red part not activated) and the hydrogen compression is planned every night at midnight (blue part).
The two proposed EMSs are then compared with an EMS characterized by hydrogen production exclusively with energy from the grid. In this case, the followed EMS is similar to the Mixed one. The only difference is that the black part is not considered (PV and BS are not present), while in the red part, the hydrogen production with energy from grid covers the whole day.

3.5 Optimization

A multi-objective optimization is formulated and solved with the goal of finding the best optimal design of the renewable-based microgrid by considering two conflicting objective functions: the maximization of the self-sufficiency rate (SSR), which indicates the microgrid ability to satisfy the HRS demand (ratio between the amount of green hydrogen produced by the HG, $\dot{m}_{HG,green}$, and the total quantity required, $\dot{m}_{HRS}$, as reported in equation (7)), and the minimization of the Levelized Cost Of Hydrogen (LCOH), reported in Equation (8), which indicates the ratio between the total expenditure and the hydrogen delivered ($H_2\ HRS_d$) to the HRS.

$$SSR = \frac{\sum_t \dot{m}_{HG,green}(t)}{\sum_t \dot{m}_{HRS}(t)} \tag{7}$$

$$LCOH = \frac{TCI + (E_{FG} + OM \cdot TCI) \cdot \sum(1+IR)^{-y}}{H_2\ HRS_d \cdot \sum(1+IR)^{-y}} \tag{8}$$

where the term TCI was calculated by Equation (9), starting from the Purchase Equipment Costs (PEC), as a function of the relative size of the hydrogen section components and their specific costs (c), listed in Table 2.

$$TCI = \left[\left(c_{PV}\ P_{PV,nom} + c_{BS}\ \frac{E_{BS,nom}}{DOD_{BS}} + c_{HG}\ P_{HG,nom}{}^{0.885} + c_{LP\ HT}\ V_{LP\ HT} + c_{HP\ HT}\ V_{HP\ HT} + c_{HC}\ P_{HC,nom}{}^{0.6038} + c_{HRS}\right)(1+c_{BOP})\right](1+c_{EC}) \tag{9}$$

Table 2: Main parameters assumed for the economic analysis (Micena et al., 2020; Serra et al., 2020).

Parameter	Value	Parameter	Value
Operating and Maintenance costs (OM)	5% TCI	Battery Storage (c_{BS})	697.5 €/kWh
Interest Rate (IR)	5%	Hydrogen generator (c_{HG})	3165.72 €/kW
Lifetime (y)	20 years	Hydrogen Compressor (c_{HC})	37 232.55 €/kW
Balance of Plant costs (c_{BOP})	10% PEC	Hydrogen tank @35 bar ($c_{HT\ LP}$)	83.69 €/m^3
Engineering costs (c_{EC})	10%	Hydrogen tank @450 bar ($c_{HT\ HP}$)	125 €/m^3
Photovoltaic (c_{PV})	1 058.34 €/kW	Hydrogen Refueling Station (c_{HRS})	158 100 €

In Equation (9), c_{BOP} are the costs for the balance of plant (expressed as a percentage of the PEC) and c_{EC} are the Engineering Costs (expressed as a percentage of the PEC+BOP costs). The optimization problem is implemented in MATLAB and solved with a multi-objective genetic algorithm, starting

https://doi.org/10.52202/077185-0008

with a population of 5000 variable combinations. The design variables to be optimized and the corresponding lower and upper bounds are: PV plant nominal power: 0 kW ÷ 3 000 kW; BS nominal capacity: 0 kWh ÷ 1 000 kWh; HG nominal power: 100 kW ÷ 1 000 kW; LP-HT geometrical volume: 10 m^3 ÷ 100 m^3; HP-HT geometrical volume: 1.1 m^3 ÷ 2 m^3.

4 RESULTS AND DISCUSSION

In this section, the annual performance of the renewable microgrid based on different EMSs are shown and discussed. In particular, the results are represented by the Pareto front resulting from the multi objective optimization. The results are then compared with the hydrogen production costs resulting by powering the HG only with the public grid, highlighting the additional costs deriving from the requirement of storage systems to guarantee the production and use of green hydrogen.

4.1 Green Hydrogen Production EMS

The Pareto front resulting from the optimization of the Green Hydrogen Production EMS is represented in Figure 3. As expected, the two objective functions conflict, since to achieve increasingly higher SSR a significant increase in the size of the microgrid components is required with a consequent rise in the total investment.

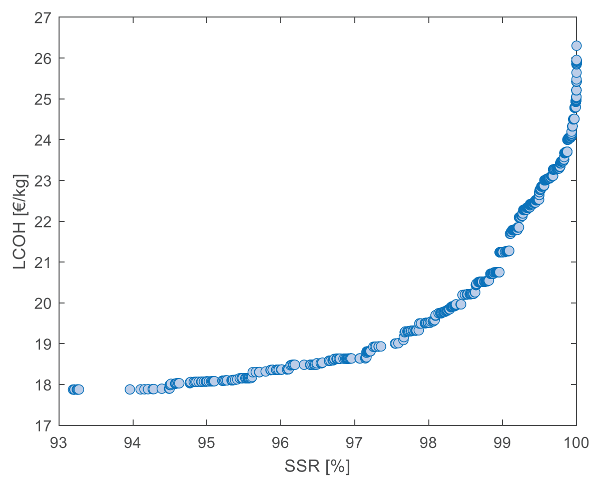

Figure 3: Pareto Chart resulting from the Green Hydrogen Production EMS

The lowest LCOH (equal to 17.88 €/kg) is obtained for microgrid configuration achieving also the lowest SSR, 93.19%, while the 100% SSR results in an increase of LCOH to 25.02 €/kg. The important increment in hydrogen production costs can be justified by comparing the design variables found for these extreme optimizations:

- Lowest LCOH: PV=1 013 kW; BS=70 kWh; HG=476 kW; LP-HT=28.4 m^3; HP-HT=1.1 m^3
- Highest SSR: PV=2 061 kW; BS=186 kWh; HG=840 kW; LP-HT=67.7 m^3; HP-HT=1.5 m^3

As can be observed, almost all components increase in size, especially PV, BS and the LP-HT, which increase their size more than double, while only the HP-HT increases to a lesser extent.

The variation in sizing of the microgrid components for all points composing the Pareto front at the increasing of the SSR is reported in Figure 4. As can be observed, the Pareto front is representative of microgrid characterized by an almost constant increase in the PV and HG nominal powers, while the BS capacity does not vary significantly. A general increase in the volume of the LP-HT to achieve increasing SSR is also observed, although the trend appears more discontinuous, while marginal variations in the volume of the HP-HT are detected.

https://doi.org/10.52202/077185-0008

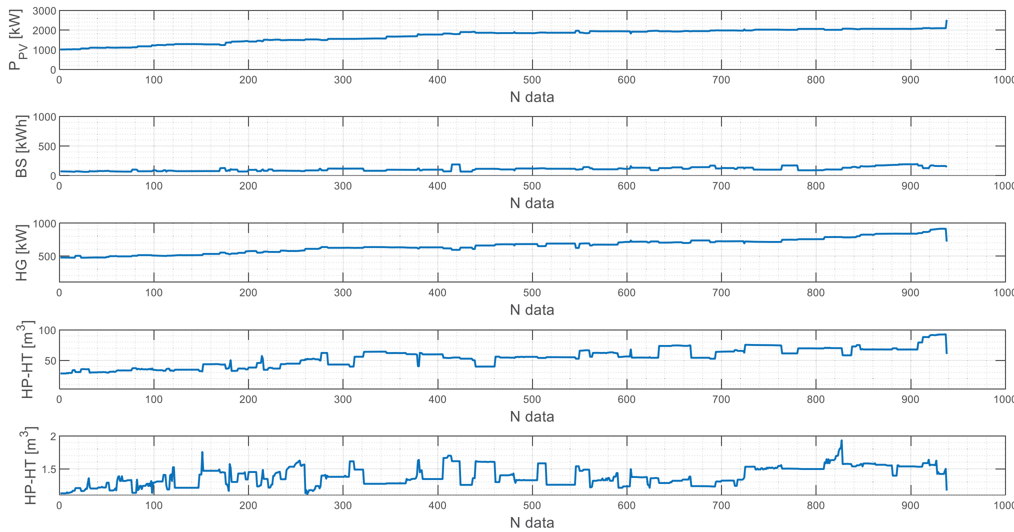

Figure 4: Sizing of renewable-based microgrid components (Green Hydrogen Production EMS)

4.2 Mixed Hydrogen Production EMS

Figure 5 and Figure 6 show the Pareto front and the corresponding size of the microgrid components, respectively, obtained by including the possibility of partially producing hydrogen by using the grid.

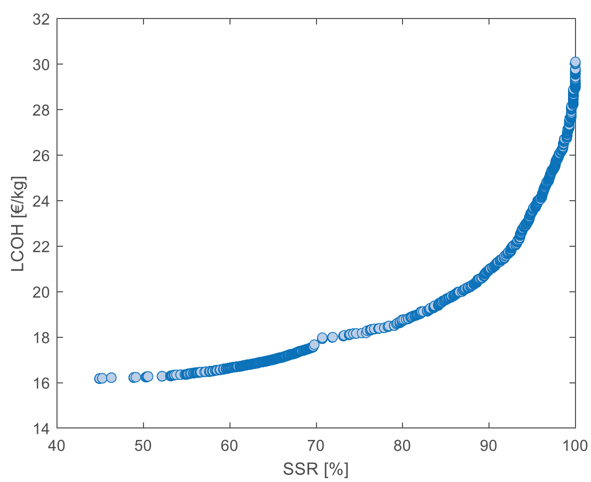

Figure 5: Pareto Chart resulting from the Mixed Hydrogen Production EMS

In this case, the SSR values are characterized by a greater range compared to the previous case. In particular, the microgrid configurations achieving the lowest LCOH (16.17 €/kg) are characterized by a low SSR (44.9%): this means that the share of hydrogen produced by RES is less than half. The 100% SSR is instead characterized by a LCOH of 28.95 €/kg, higher than that obtained in the previous case. The size of the components for these two extreme cases are:

- Lowest LCOH: PV=532 kW; BS=63 kWh; HG=409 kW; LP-HT=16.2 m^3; HP-HT=1.6 m^3
- Highest SSR: PV=2 538 kW; BS=114 kWh; HG=729 kW; LP-HT=63.5 m^3; HP-HT=1.16 m^3

The difference between the size is evident for all components, and only the HP-HT see a reduction in its size. As can be noticed, two different parts can be analyzed: the first is characterized by a SSR up to values close to 70% (Figure 5), while the second one after the latter point. In the first part the design parameters (Figure 6) are almost constant and similar to the lowest values (lowest LCOH),

https://doi.org/10.52202/077185-0008

except for a slight increase in the PV nominal power and HP-HT volume. A different trend characterizes the second part, where an increase in size for the PV and HG can be observed, while BS remain almost in the same range as before. Regarding the HTs, these are characterized by an opposite trend: the LP-HT size increases in a jagged way to decrease in the last point, while the HP-HT decrease to its lower value until the last points, where increase.

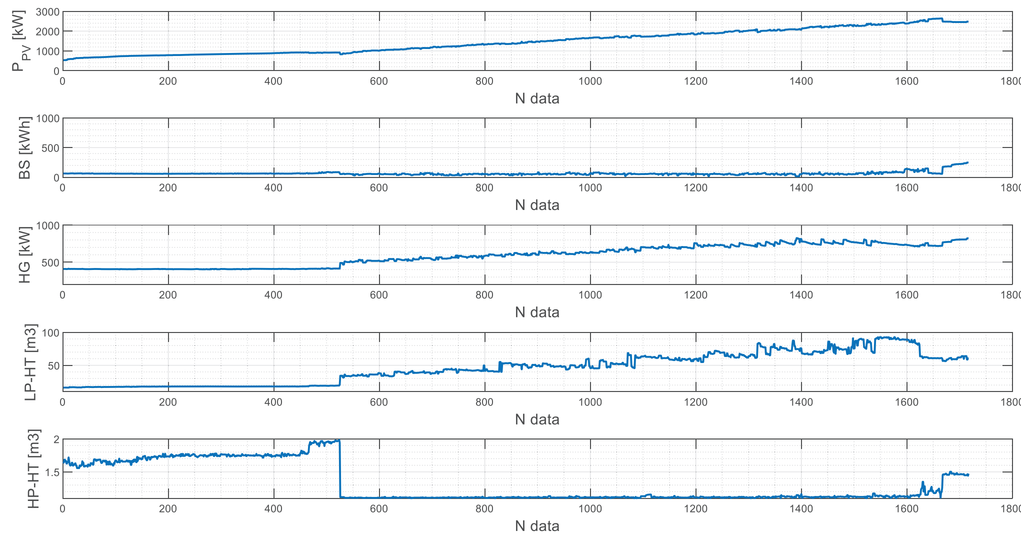

Figure 6: Sizing of renewable-based microgrid components (Mixed Hydrogen Production EMS)

4.3 Comparison with microgrid powered by the grid

The performance obtained for the two proposed EMS are finally compared with the performance achieved by an HRS fed by an HG exclusively powered by the grid. Since no green hydrogen production is produced in this case, the sole minimization of the LCOH is pursued during the optimization process. The LCOH found in this case is 13.37 €/kg, with a HG of 205.2 kW, a LP-HT of 15 m^3 and a HP-HT of 1.1 m^3 (PV and BS are not present). A summary of the results found for each EMS is reported in Table 3.

Table 3: Results summary of all Energy Management Strategies

	SSR [%]	LCOH [€/kg]	PV [kW]	BS [kWh]	HG [kW]	HT_LP [m^3]	HT_HP [m^3]	H_2 from GRID [%]	CO_2 emissions [t CO_2/year]
GREEN-EMS	93.19	17.88	1 013	70	476	28.4	1.1	-	-
	99.25	*22.13*	*1 897*	*67*	*628*	*52.7*	*1.25*	-	-
	100	**25.02**	**2 061**	**186**	**840**	**67.7**	**1.5**	**-**	**-**
MIXED-EMS	44.9	16.17	532	63	409	16.2	1.6	55.1	300.08
	70.7	17.92	830	54	490	34.2	1.1	29.3	170.41
	93.21	*22.12*	1 576	85	614	45.3	1.3	6.79	52.56
	100	**28.95**	**2 538**	**114**	**729**	**63.5**	**1.16**	**-**	**17.18**
GRID-EMS	**-**	**13.37**	**-**	**-**	**205.2**	**15**	**1.1**	**100**	**532.22**

In particular, the values obtained for the two objective functions are reported together with the sizing of the main microgrid component and the percentage of hydrogen produced by electricity from the grid. The table also reports the CO_2 emissions per year of the different cases, obtained by multiplying

https://doi.org/10.52202/077185-0008

the annual amount of electricity purchased from the public grid with the average emissions factor for electricity production registered in Italy in 2022, equal to 0.331 kg CO_2/kWh (Terna spa., 2024).

Considering the results obtained for the microgrid with a SSR equal to 100% (in bold), comparing the results obtained with a Green Hydrogen Production EMS (GREEN-EMS) and with a mixed one (MIXED-EMS) the values found for the LCOH and for the components are similar, with a slightly lower LCOH value found for the case of GREEN-EMS (25.02 €/kg vs 28.95 €/kg) due to the lower PV size. Otherwise, looking at the results obtained for the lowest LCOH, the lowest value was found for the MIXED-EMS (16.17 €/kg vs 17.88 €/kg). However, the SSR for the MIXED-EMS is in this case lower than that found for the GREEN-EMS: in fact, while with the GREEN-EMS the SSR is about 93% (but the remaining 7% is not satisfied), for the mixed case the value decreases up to 45%, while the remain HRS demand is satisfied with hydrogen produced by using the public grid (55%). Looking at the components size, for the MIXED-EMS these are lower, especially the PV size: this means that the other costs are due to the energy purchased from the grid. Two other cases were analyzed for the MIXED-EMS: one considering the microgrid configuration characterized by a LCOH close to that found for the GREEN-EMS (17.92 €/kg, in blue) and the other, similarly, considering the most similar SSR (93.21%, in red). For the first case, the SSR is lower that the value found for the GREEN-EMS (70.7% vs 93.19%), due to the smaller components size of the renewable section (PV+BS), while the second case, with a SSR similar between the different EMS, is characterized by a higher LCOH of the MIXED-EMS (22.12 €/kg vs 17.88 €/kg), due both to the higher components size and the energy taken from the grid. Finally, starting from the MIXED-EMS point with a LCOH of 22.12 €/kg, the point of the GREEEN-EMS with the same cost was analyzed (highlighted in yellow): a SSR of 99.25% was therefore found. In this case, both parity was found in terms of LCOH and total SSR: however, since in the GREEN-EMS a greater renewable SSR was found (99.25% vs 93.21%), this solution is preferable. As expected, the lowest LCOH is obtained by producing hydrogen directly from electricity purchased from the grid, i.e. 13.37 €/kg. In this case, the hydrogen generator is not limited by the capacity factor of the PV system and it can operate continuously, resulting in a downsizing of this component thanks to its greater utilization factor and a strong reduction of the hydrogen storage capacity required. However, as expected, this case is also characterized by higher emissions, almost double compared to the use of diesel buses (532.22 t CO_2/year vs 284.46 t CO_2/year). Emissions are instead equal to zero for the cases relating to the GREEN-EMS, while they increase as the renewable SSR decreases in the MIXED-EMS cases. Even for this last strategy, in the case characterized by the lowest LCOH, it is not convenient to replace the vehicles from the point of view of emissions (300.08 t CO_2/year, slightly higher than the case with diesel vehicles).

A particular note must be made on the costs obtained: these, in fact, are higher than those commonly found in the literature (between 2.6 and 12.3 €/kg, according to (Guerra *et al.*, 2019). However, some important aspects of the case study analyzed should be underlined: the renewable-based microgrid is exclusively used for the refueling station, that is, the PV energy production is limited by the current HG demand. Furthermore, the cost is strongly influenced by the production of hydrogen, which is rather low (approximately 26.5 t/year), which means a low utilization factor of the HG with a consequent high impact in the initial costs. A solution to lower costs could therefore be replace a greater number of buses, thus increasing annual hydrogen production.

5 CONCLUSIONS

In this study, a techno-economic assessment was carried out on the integration of a HRS into a renewable-based microgrid, with the aim of replacing six diesel buses with hydrogen vehicles in one line of the local transport company of Cagliari (Italy). A mathematical model was implemented in MATLAB to study the annual energy performances of the proposed microgrid, while three EMSs were proposed to study the performances with an increasing green hydrogen production. The microgrid design was optimized based on a multi-objective genetic algorithm, in order to maximize the self-sufficiency of the HRS and minimizing the LCOH.

The results showed that, as expected, the lowest LCOH, equal to 13.37 €/kg, is achieved if hydrogen is produced only with electricity from the grid. This is due to the absence of the renewable section

https://doi.org/10.52202/077185-0008

(PV+BS) and to the smaller size requested for the hydrogen generator and storage section. However, this is also the case characterized by greater CO_2 emissions, which are almost double those obtained from diesel vehicles. On the other hand, the production of green hydrogen by means of a renewable based microgrid that operate with a self-sufficiency equal to 100% results in a double of the hydrogen costs: the LCOH ranges from 25.02 €/kg of the green hydrogen production EMS to 28.95 €/kg of the mixed hydrogen production EMS. This increase is due not only to the inclusion of the renewable section, but also to the strong increase in the sizes of HG and LP-HT, which more than triple their dimensions. Furthermore, considering the results with the same SSR and LCOH, it was found that starting from an LCOH of 22.12 €/kg the best EMS is the Green-EMS, which guarantees a renewable SSR of 99.25% against 93.21% (with the remaining part guaranteed instead by hydrogen produced by the network). This would guarantee lower costs compared to the previously mentioned values, obtaining an SSR close to 100% and zero GHG emissions, unlike the mixed case.

NOMENCLATURE

Symbols					
DOD	Depth of Discharge	(-)	SOC	State Of Charge	(%)
E	Energy	(Wh)	t	Time	(h)
h	Enthalpy	(J/kg)	T	Temperature	(°C)
$\dot{m}$	Mass Flow Rate	(kg/s)	V	Volume	(m^3)
OM	Operating and Maintenance cost	(€)	γ	Temperature Coefficient	(-)
P	Electric Power	(W)	η	Efficiency	(-)
Subscripts					
BS	Battery Storage		*NOCT*	Nominal Operating Cell Temperature	
H_2	Hydrogen		*nom*	Nominal Conditions	
HP	High Pressure		*STC*	Standard Test Conditions	
LP	Low Pressure		*y*	Years	
Acronyms					
BEV	Battery Electric Vehicle		GHG	Greenhouse Gases	
DB	Diesel Buses		PEM	Proton Exchange Membrane	
FCEV	Fuel Cell Electric Vehicle		WT	Wind Turbine	

REFERENCES

Bahou, S. (2023). Techno-economic assessment of a hydrogen refueling station powered by an on-grid photovoltaic solar system: A case study in Morocco. *International Journal of Hydrogen Energy*, *48*(61), 23363–23372. https://doi.org/10.1016/J.IJHYDENE.2023.03.220

Cardona, P., Costa-Castell, R., Roda, V., Carroquino, J., Vali, L., Ocampo-Martinez, C., & Serra, M. (2023). *Modelling and operation strategy approaches for on-site Hydrogen Refueling Stations*. https://doi.org/10.1016/j.ijhydene.2023.08.192

Coppola, P., Bocciolone, M., Colombo, E., De Fabiis, F., & Sanvito, F. D. (2023). Multi-Criteria Life-Cycle Assessment of bus fleet renewal: A methodology with a case study from Italy. *Case Studies on Transport Policy*, *13*, 101044. https://doi.org/10.1016/J.CSTP.2023.101044

Duffie, J. A., & Beckman, W. A. (2013). Solar Engineering of Thermal Processes: Fourth Edition. *Solar Engineering of Thermal Processes: Fourth Edition*. https://doi.org/10.1002/9781118671603

Estrada Poggio, A., Balest, J., Zubaryeva, A., & Sparber, W. (2023). Monitored data and social perceptions analysis of battery electric and hydrogen fueled buses in urban and suburban areas. *Journal of Energy Storage*, *72*, 108411. https://doi.org/10.1016/J.EST.2023.108411

https://doi.org/10.52202/077185-0008

Förster, R., Kaiser, M., & Wenninger, S. (2023). Future vehicle energy supply - sustainable design and operation of hybrid hydrogen and electric microgrids. *Applied Energy*, *334*, 120653. https://doi.org/10.1016/J.APENERGY.2023.120653

Fragiacomo, P., Genovese, M., Piraino, F., Corigliano, O., & De Lorenzo, G. (2022). Hydrogen-Fuel Cell Hybrid Powertrain: Conceptual Layouts and Current Applications. *Machines*, *10*(12). https://doi.org/10.3390/MACHINES10121121

Gökçek, M., & Kale, C. (2018). Optimal design of a Hydrogen Refueling Station (HRFS) powered by Hybrid Power System. *Energy Conversion and Management*, *161*, 215–224. https://doi.org/10.1016/J.ENCONMAN.2018.02.007

Grazieschi, G., Zubaryeva, A., & Sparber, W. (2023). Energy and greenhouse gases life cycle assessment of electric and hydrogen buses: A real-world case study in Bolzano Italy. *Energy Reports*, *9*, 6295–6310. https://doi.org/10.1016/J.EGYR.2023.05.234

Guerra, O.J., Eichman, J., Kurtz, J., Hodge, B.M. Cost Competitiveness of Electrolytic Hydrogen. (2019). *Joule*. *3, 2425-2443*. https://doi.org/10.1016/j.joule.2019.07.006

Hanlon P.C. (2001). Compressor Handbook. *McGraw-Hill*.

Kakoulaki, G., Kougias, I., Taylor, N., Dolci, F., Moya, J. & Jäger-Waldau, A. (2021). Green hydrogen in Europe – A regional assessment: Substituting existing production with electrolysis powered by renewables. *Energy Conversion and Management*, *228*, 113649, https://doi.org/10.1016/j.enconman.2020.113649

Lawrence, O. O., Ikechi, N. N., & John, O. E. (2023). Techno-economic investigation of hybrid peaker plant and hydrogen refueling station. *International Journal of Hydrogen Energy*. https://doi.org/10.1016/J.IJHYDENE.2023.09.198

Logan, K. G., Nelson, J. D., & Hastings, A. (2020). Electric and hydrogen buses: Shifting from conventionally fueled cars in the UK. *Transportation Research Part D: Transport and Environment*, *85*, 102350. https://doi.org/10.1016/J.TRD.2020.102350

Maestre, V. M., Ortiz, A., & Ortiz, I. (2023). Decarbonizing the Spanish transportation sector by 2050: Design and techno-economic assessment of the hydrogen generation and supply chain. *International Journal of Hydrogen Energy*, *48*(99), 39514–39530. https://doi.org/10.1016/J.IJHYDENE.2023.05.154

Mallapragada, D.S., Gençer, E., Insinger, P., Keith, D.W., O'Sullivan, F.M. (2020). Can Industrial-Scale Solar Hydrogen Supplied from Commodity Technologies Be Cost Competitive by 2030?. *Cell Reports Physical Science*, https://doi.org/10.1016/j.xcrp.2020.100174.

Meteonorm. Retrieved January 5, 2024, from https://meteonorm.com/en/

Micena, R. P., Llerena-Pizarro, O. R., de Souza, T. M., & Silveira, J. L. (2020). Solar-powered Hydrogen Refueling Stations: A techno-economic analysis. *International Journal of Hydrogen Energy*, *45*(3), 2308–2318. https://doi.org/10.1016/J.IJHYDENE.2019.11.092

Pang, Y., Pan, L., Zhang, J., Chen, J., Dong, Y., & Sun, H. (2022). *Integrated sizing and scheduling of an off-grid integrated energy system for an isolated renewable energy hydrogen refueling station*. https://doi.org/10.1016/j.apenergy.2022.119573

Schnuelle, C., Wassermann, T., Fuhrlaender, D. & Zondervan, E. (2020). Dynamic hydrogen production from PV & wind direct electricity supply – Modeling and techno-economic assessment. *International Journal of Hydrogen Energy*. 45(55), 29938-29952. https://doi.org/10.1016/j.ijhydene.2020.08.044

Serra, F., Lucariello, M., Petrollese, M., & Cau, G. (2020). *Optimal Integration of Hydrogen-Based Energy Storage Systems in Photovoltaic Microgrids: A Techno-Economic Assessment*. https://doi.org/10.3390/en13164149

SUNPOWER MAXEON 3 SOLAR PANEL 355-375 W. Retrieved January 16, 2024, from https://sunpower.maxeon.com/uk/sites/default/files/2022-05/sp_max3_104c_blk_375-355_dc_ds_en_a4_544453.pdf

Terna spa. - Production: Electricity by source. Retrieved May 16, 2024, from https://www.terna.it/en/electric-system/statistical-data-forecast/evolution-electricity-market/production-electricity-source

https://doi.org/10.52202/077185-0008